NANO LETTERS

Letter

pubs.acs.org/NanoLett

Kondo Effect of Cobalt Adatoms on a Graphene Monolayer Controlled by Substrate-Induced Ripples

Jindong Ren,[†,#] Haiming Guo,[†,#] Jinbo Pan,[†,#] Yu Yang Zhang,[‡,⊥,#] Xu Wu,[†] Hong-Gang Luo,[§,∥] Shixuan Du,[†] Sokrates T. Pantelides,*[,‡,⊥] and Hong-Jun Gao*[,†]

[†]Institute of Physics, Chinese Academy of Sciences, Beijing 100190, China

[‡]Department of Physics and Astronomy, Vanderbilt University, Nashville, Tennessee 37240 United States

[§]Center for Interdisciplinary Studies and Key Laboratory for Magnetism and Magnetic Materials of the MoE, Lanzhou University, Lanzhou 730000, China

[∥]Beijing Computational Science Research Center, Beijing 100084, China

[⊥]Materials Science and Technology Division, Oak Ridge National Laboratory, Oak Ridge, Tennessee 37831, United States

Supporting Information

ABSTRACT: The Kondo effect, a widely studied phenomenon in which the scattering of conduction electrons by magnetic impurities increases as the temperature T is lowered, depends strongly on the density of states at the Fermi energy. It has been predicted by theory that magnetic impurities on free-standing monolayer graphene exhibit the Kondo effect and that control of the density of states at the Fermi level by external means can be used to switch the effect on and off. However, though transport data for Co adatoms on graphene monolayers on several substrates have been reported, there exists no evidence for a Kondo effect. Here we probe the role of the substrate on the Kondo effect of Co on graphene by combining low-temperature scanning tunneling microscopy and spectroscopy measurements with density functional theory calculations. We use a Ru(0001) substrate that is known to cause graphene to ripple, yielding a moiré superlattice. The experimental data show a sharp Kondo resonance peak near the Fermi energy from only Co adatoms at the edge of atop regions of the moiré pattern. The theoretical results show that the variation of the distance from the graphene to the Ru substrate, which controls the spin polarization and local density of states at the Fermi energy, is the key factor for the appearance of the Kondo resonance. The results suggest that rippling of graphene by suitable substrates is an additional lever for tuning and selectively switching the appearance of the Kondo effect.

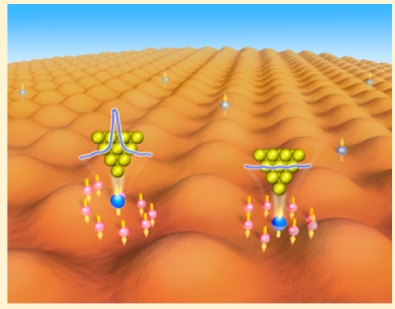

KEYWORDS: *Kondo effect, scanning tunneling microscopy, graphene, magnetic impurity, surface adsorption*

The Kondo effect arises from the coupling of a localized spin with the surrounding conduction electrons in dilute magnetic alloys or on magnetic adatoms at surfaces.[1,2] The effect leads to a rise in resistivity as the temperature is lowered and produces a narrow electronic resonance at the Fermi level below the Kondo temperature (T_K). This resonance is a manifestation of strong electron correlations, whereby the Kondo effect has drawn significant attention in the past 50 years. Since the invention of scanning tunneling microscopy and spectroscopy (STM/STS), the Kondo effect has been intensively investigated by this technique, ranging from observing to manipulating single magnetic atoms or molecules on different substrates.[3−14] Effects of adsorption and supporting substrates are well established.[7−10]

The Kondo temperature T_K, which reflects the strength of the coupling between itinerant electrons and the localized spin of a magnetic impurity, is proportional to $\exp(-1/J\rho_F)$. ρ_F is the product of the density of states at the Fermi energy and J is the magnetic coupling. The latter depends on the spin polarization (magnetic moment) of the magnetic impurity. Graphene has a unique energy-band structure with the Fermi energy at the point of a "Dirac cone", which allows one to make large changes in ρ_F by shifting the Fermi energy easily by external means.[15−17] In particular, one can move the Fermi energy significantly in either direction by applying a gate bias. Theoretical calculations found that the Kondo effect arising from magnetic impurities, for example, Co, on graphene can be turned on and off by such changes of the Fermi energy.[18−22] Experimentally, the magnetic and transport properties of various magnetic-impurity-on-graphene systems, for example, Co/G/SiC(0001),[23] Co/G/SiO_2/Si,[24,25] and Co/G/Pt(111),[26] have been studied. The published data, however, do not contain any evidence for a Kondo effect.

In this paper, we report the first observation of the Kondo effect caused by Co adatoms on the graphene/Ru(0001) system. The choice of the substrate was motivated by the fact that the distance between graphene and Ru substrate is strongly modulated by the moiré pattern, which yields a variety of local

Received: April 16, 2014
Revised: June 4, 2014
Published: June 6, 2014

electronic structures in the G/Ru(0001) system. By measuring dI/dV STS spectra from individual Co atoms, we find that only Co atoms on the two nonequivalent edges of so-called atop regions of the moiré pattern, which are an intermediate distance from the Ru substrate, give rise to a narrow resonance around the Fermi energy (E_F). Zeeman splittings were measured using magnetic-field-dependent STS spectra to verify that the observed resonance is indeed produced by the Kondo effect. Temperature-dependent spectra were measured and Kondo temperatures equal to 12.10 ± 0.10 and 5.39 ± 0.06 K were extracted for two types of adsorption sites. Theoretical results obtained by density functional calculations show that the distance of the graphene in the region of each Co adatom to the Ru substrate controls the spin polarization of the Co adatoms and the local density of states at the Fermi energy of the host material. The results correlate well with the experimental data. As a final test, silicon atoms were intercalated between the graphene and the Ru substrate, which flattens the graphene at a larger distance. As in the case of flat graphene on other substrates, no Kondo effect is observed (ρ_F is essentially zero as in free-standing graphene).

Experiments were performed using an ultrahigh vacuum (UHV) LT-STM system (Unisoku) with a base pressure better than 2×10^{-10} mbar. The Ru(0001) crystal was prepared by repeated cycles of Ar^+ sputtering and annealing up to 1500 K. Graphene was fabricated by thermal decomposition of ethylene on the Ru(0001) surface. Co was deposited from a cobalt rod (purity of 99.99%) onto the G/Ru(0001) system at the substrate temperature of ~20 K using a commercial electron beam evaporator. The sample was then transferred into the STM head which can operate at 0.5 or 4.2 K. STM images were acquired in the constant-current mode. The bias voltage was applied to the sample with respect to the tip. Spectroscopic measurements were recorded by using a lock-in technique with a modulation voltage of 0.03 mV rms sinusoidal at a frequency of 973 Hz. All tip states were calibrated on bare graphene before and after measurements to ensure that there are no tip-related features on the recorded dI/dV spectra. A magnetic field up to B = 8.6 T was applied perpendicularly to the sample surface.

Density functional theory (DFT)-based first-principles calculations were performed using the Vienna ab initio simulation package (VASP).[27] Projector augmented wave (PAW) potentials were used to describe the core electrons,[28] and the local density approximation (LDA) was used for exchange and correlation.[29] The periodic slab models include two layers of 11 × 11 ruthenium, one layer of 12 × 12 graphene, and a vacuum layer of 18 Å. The energy cutoff of the plane-wave basis sets was 450 eV, and the Brillion zone was sampled at the Γ point. All atoms were fully relaxed except for the bottom ruthenium atoms until the net force on every atom was less than 0.01 eV/Å.

After deposited on graphene/Ru(0001), Co adatoms adsorbed at several distinct sites. The highly ordered moiré structure of epitaxial monolayer graphene that forms on the Ru(0001) surface is usually divided into three distinct regions in terms of the local distance to Ru substrate,[30,31] that is, fcc, hcp, and atop regions, as shown in Figure 1a. Among these three regions, there is an apparent height difference of ~0.10 nm as measured using STM. When the Co atoms are deposited onto G/Ru(0001) at low temperature (~20 K), three Co adsorption species were distinguished by their location with respect to the site of the graphene moiré pattern on Ru(0001):

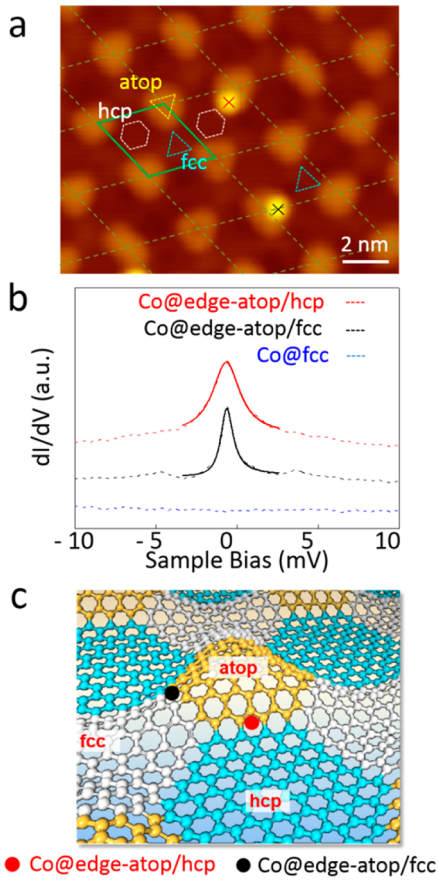

Figure 1. (a) STM topography presenting two Co atoms adsorbed on G/Ru(0001) system with different locations with respect to the moiré pattern sketched in green dash lines. (b) Spectroscopic measurements (T = 0.5 K with the tunneling parameters: I = −0.2 nA; V_b = −0.04 V; modulation, 0.03 mV/973 Hz) taken on Co adatoms shown in (a). The dash lines are the experiment data while the solid lines are the corresponding Fano fit results. The STS curve observed on Co@edge-atop/fcc shows a Kondo resonance with a narrower width than that on Co@edge-atop/hcp. STS on Co@fcc shows no Kondo resonance. (c) A schematic to illustrate the adsorption site of Co@edge-atop/fcc and Co@edge-atop/hcp.

Co@hcp for Co atoms adsorbed on hcp regions, Co@fcc for Co atoms adsorbed on fcc regions, and Co@edge-atop for Co atoms adsorbed on the edge of the atop regions. By performing a statistical analysis of several hundred Co adsorption sites obtained from STM images, we found that more than half of Co adatoms are adsorbed at the edge of atop regions (56.3%), 33% of the Co adatoms are adsorbed at the fcc regions, and 10.4% are adsorbed at hcp regions. Furthermore, for Co@edge-atop, the Co adatoms can be divided into two different species: facing to the fcc side (labeled as Co@edge-atop/fcc) or to the hcp side (labeled as Co@edge-atop/hcp). A schematic of the adsorption sites is shown in Figure 1c.

The dI/dV curves were taken on the Co adatoms at different adsorption sites (shown in Figure 1b). For Co@fcc or Co@hcp adatom, a smooth and featureless curve is obtained around E_F. In contrast, a sharp peak at E_F is present in the spectra obtained from Co@edge-atop. The sharp peak at E_F can be attributed to the Kondo effect based on its magnetic field-dependent (Figure 2) and temperature-dependent (Supporting Information Figure S2) measurements. The Kondo peak is narrower for Co@edge-atop/fcc than that of the Co@edge-atop/hcp. By using the

dx.doi.org/10.1021/nl501425n | Nano Lett. 2014, 14, 4011−4015

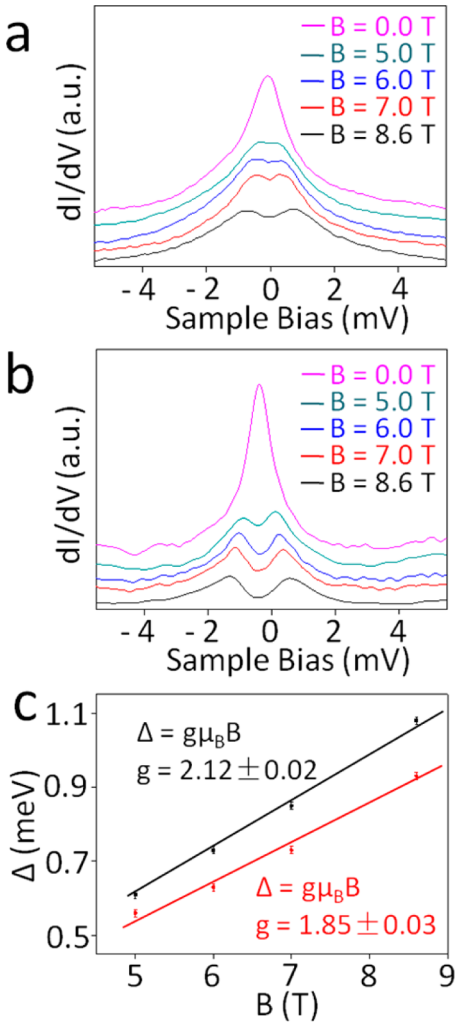

Figure 2. Magnetic-field dependent on the Kondo resonance for (a) Co@edge-atop/hcp and (b) Co@edge-atop/fcc, the Kondo peaks are split in magnetic field. (c) Magnetic field dependent on the Zeeman energy with different g factor for Co adatom facing to different site. The red curve is for Co@edge-atop/hcp, and the black curve is for Co@edge-atop/fcc. All dI/dV spectra were performed at T = 0.5 K with the tunneling parameters: I = −0.2 nA, V_b = −0.04 V; modulation, 0.03 mV/973 Hz.

Fano-Lorentz function, the Kondo temperatures at these two adsorption sites are fitted as 5.39 ± 0.06 and 12.10 ± 0.10 K, respectively. Although the Fano-Lorentz fits may overestimate the Kondo temperature compared with the Frota function fits according to ref 32, it is more popularly used for magnetic adatom/molecule on the surfaces[6−9,33] while the latter is often used for the magnetic impurity alloy system.[34,35] With both these fitting methods, the comparative analysis of the Kondo temperatures of Co adatoms on these two adsorption sites can be clearly established. Spatially dependent measurements show the spatial dependence of the Kondo resonance of Co adatom on graphene (Figure 3). The intensity of the Kondo peak decreases monotonically when the dI/dV measurement is performed at the position away from the center of Co adatom. This behavior is similar to the observed Co atoms on the metal surfaces.[4,7] The peak eventually disappears over a lateral distance of about 1 nm, which indicates the upper limit of the influence radius of the magnetic impurity on the LDOS of graphene at this experimental condition.

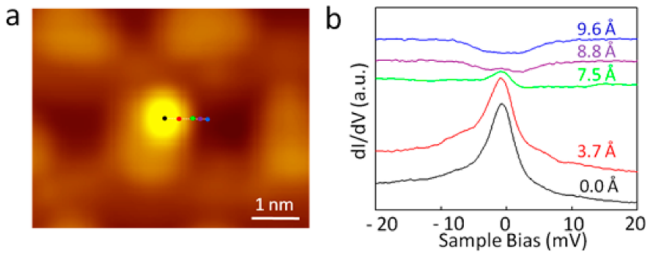

Figure 3. Lateral dependence of Kondo resonance line shape taken from the center of single Co atom on G/Ru(0001) surface. (a) Topography of single Co adatom sited on the edge of atop region of G/Ru(0001). (b) Spectra measurements taken away from the center of Co adatom (see (a)). (Each curve has been shifted vertically for viewing, T = 4.2 K, tunneling parameters: I = −0.1 nA, V_b = −0.08 V).

To further investigate the two kinds of Kondo resonance for Co atoms at different edge sites, magnetic-field-dependent measurements were performed. Figure 2a,b shows the evolution of the spectra taken at 0.5 K with an applied magnetic field perpendicular to the sample surface. A splitting of the Kondo resonance peaks for Co@edge-atop/hcp and Co@edge-atop/fcc is observed under an external magnetic field. For these cases, Zeeman splitting with a dip-shaped feature in dI/dV spectra appears in the center of the Kondo resonance peaks close to the Fermi level. These results further confirm that the peaks are Kondo resonances. The Zeeman splitting energy varies linearly with the magnetic field. We get values of g factor of about 2.12 ± 0.02 for Co@edge-atop/fcc and 1.85 ± 0.03 for Co@edge-atop/hcp by fitting to the formula $\Delta = g\mu_B B$ (where μ_B is the Bohr magneton) (see Figure 2c).

The site-specific magnetic properties of Co adatoms on G/Ru(0001) system can be understood by the results of DFT calculations. In Table 1, we show the distance of the Co adatom

Table 1. Theoretical Calculation Results of Co Adsorption on Different Sites of G/Ru(0001) Surface[a]

		edges-atop			
	atop	/hcp	/fcc	fcc	hcp
d/nm	0.51	0.46	0.47	0.40	0.37
E_b/eV	4.20	4.30	4.28	4.28	3.91
μ/μ_B	1.0	1.0	1.0	0.6	0.0
LDOS/au	0.1	0.8	0.7	1.8	1.2
T_K/K		12.10 ± 0.10	5.39 ± 0.06		

[a] d is the vertical distance between Co adatom from the Ru substrate. E_b is the binding energy. μ is the magnetic moments. LDOS is the summation of locally density of states of the six carbon atoms under the Co adatom. T_K is the Kondo temperature derived from experiments.

from the substrate, the binding energies, and magnetic moments of Co adatoms at the four different sites and the local electron density of the nearest six carbon atoms at the Fermi energy at each site. It is clear that the results correlate well with the experimental data. Both the two edge-atop sites have a large magnetic moment, which suggests large coupling to the itinerant electron spins, and have a substantial local density of states at the Fermi energy. These are the sites that exhibit a Kondo resonance. The hcp site has zero magnetic moment and thus has no Kondo effect, as observed. The fcc site has intermediate values of magnetic moment and large ρ_F, which do

dx.doi.org/10.1021/nl501425n | Nano Lett. 2014, 14, 4011−4015

not give a definitive indication of the Kondo status. The above results make it clear that at the larger graphene−substrate distances, the Kondo effect is quenched by the near-zero ρ_F, as in free-standing graphene. At the smaller distances, ρ_F is large but the magnetic moment is quenched by the chemical bonding and rehybridization of the Co orbitals.

According to Table 1, the two sites that exhibit the Kondo effect have slightly different ρ_F and slightly different Kondo temperatures. As expected, the lower Kondo temperature corresponds to the smaller ρ_F, which implies smaller magnetic coupling between the Co electrons and the itinerant electrons.

As a another check of the results described so far, we intercalated a single layer of silicon atoms between graphene and the Ru substrate to demonstrate the importance of distance from graphene to substrate. A single layer of silicon atoms was first intercalated between G/Ru(0001) interface[36] and then Co adatoms were deposited on the top graphene layer under the same experimental conditions. Figure 4a shows the topography

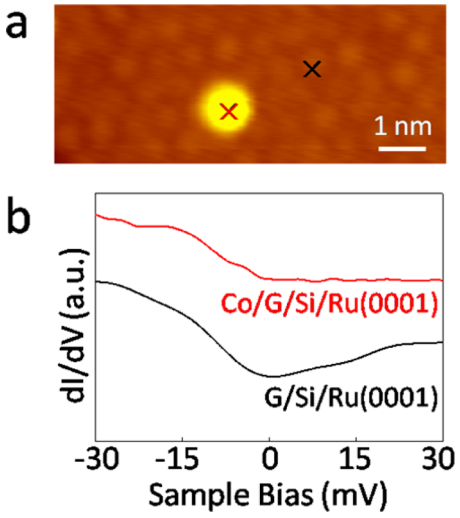

Figure 4. (a) Topography of a single Co adatom on G/Si/Ru(0001) surface. (b) dI/dV spectra of a Co adatom on G/Si/Ru(0001) surface (red line) and of the bare G/Si/Ru(0001) background (black line). STS were performed at T = 4.2 K and the tunneling parameters: I = −0.1 nA, V_b = −0.08 V; modulation, 0.5 mV/973 Hz.

image of individual Co adatoms on G/Si/Ru(0001). After the intercalation, the corrugation of moiré pattern for G/Ru(0001) changes to a $\sqrt{7} \times \sqrt{7}$, and the interaction between graphene and Ru(0001) substrate is weakened. dI/dV spectra on bare graphene and Co adatoms are shown in Figure 4b. The dI/dV spectra taken at bare graphene, which reflects the DOS,[37] decreases significantly at the Fermi level and is similar to that of the freestanding graphene. Because of the low DOS around the Fermi energy, the Kondo resonance of the Co adatom is no longer observed at this temperature.

In conclusion, for the first time we observed the Kondo effect of Co adatoms on graphene at a Ru(0001) surface by using STM/STS experiments. We find that the Kondo effect is site-specific: only Co atoms adsorbed on the edge sites of atop regions show Kondo signals. DFT calculations indicate that the Co magnetic moments and the local density of states at the Fermi energy are quite different at different sites in the rippled graphene monolayer and control the appearance of the Kondo effect. The importance of graphene−substrate interactions that can change the LDOS of graphene is also demonstrated by silicon intercalation experiments. We find that the intercalation of silicon atoms weakens the interaction between graphene and substrate and makes the DOS at the Fermi energy vanish as in freestanding graphene, quenching the Kondo effect.

■ ASSOCIATED CONTENT

Ⓢ Supporting Information

Site and size dependence of Kondo resonance of Co on G/Ru(0001), a typical fitting for obtaining q and T_K, temperature dependence of Kondo resonance width, picking up Co atoms from graphene by STM tip, Kondo resonance of Co adatom on Ru(0001) with STS measurement, Figures S1−S4. This material is available free of charge via the Internet at http://pubs.acs.org.

■ AUTHOR INFORMATION

Corresponding Authors

*E-mail: hjgao@iphy.ac.cn (H.J.G.).
*E-mail: pantelides@vanderbilt.edu (STP).

Author Contributions

#J.R., H.G., J. P., and Y.Y.Z contributed equally to this work.

Notes

The authors declare no competing financial interest.

■ ACKNOWLEDGMENTS

Work in China and YYZ were supported by National Natural Science Foundation of China (Grants 51210003, 61390500, 61274011, 11325417), National "973" projects of China (Grants 2011CB309703, 2013CBA01600), the Chinese Academy of Sciences, and Shanghai supercomputer center. STP's work at ORNL was supported by U.S. DOE Office of Basic Energy Sciences and at Vanderbilt by the McMinn Endowment. Computations by YYZ were supported by the XSEDE Science Gateways and by NERSC, which is funded by the U.S. DOE.

■ REFERENCES

(1) Kouwenhoven, L.; Glazman, L. *Phys. World* **2001**, *14*, 33.
(2) Ternes, M.; Heinrich, A. J.; Schneider, W. D. *J. Phys.: Condens. Matter* **2009**, *21*, 053001.
(3) Li, J.; Schneider, W.-D.; Berndt, R.; Delley, B. *Phys. Rev. Lett.* **1998**, *80*, 2893.
(4) Madhavan, V.; Chen, W.; Jamneala, T.; Crommie, M. F.; Wingreen, N. S. *Science* **1998**, *280*, 567.
(5) Manoharan, H. C.; Lutz, C. P.; Eigler, D. M. *Nature* **2000**, *403*, 512.
(6) Zhao, A. D.; et al. *Science* **2005**, *309*, 1542.
(7) Knorr, N.; Schneider, M. A.; Diekhöner, L.; Wahl, P.; Kern, K. *Phys. Rev. Lett.* **2002**, *88*, 096804.
(8) Wahl, P.; Diekhöner, L.; Schneider, M. A.; Vitali, L.; Wittich, G.; Kern, K. *Phys. Rev. Lett.* **2004**, *93*, 176603.
(9) Gao, L.; et al. *Phys. Rev. Lett.* **2007**, *99*, 106402.
(10) Fu, Y.-S.; et al. *Phys. Rev. Lett.* **2007**, *99*, 256601.
(11) Otte, A. F.; Ternes, M.; von Bergmann, K.; Loth, S.; Brune, H.; Lutz, C. P.; Hirjibehedin, C. F.; Heinrich, A. J. *Nat. Phys.* **2008**, *4*, 847.
(12) Franke, K. J.; Schulze, G.; Pascual, J. I. *Science* **2011**, *332*, 940.
(13) Choi, D.-J.; Rastei, M. V.; Simon, P.; Limot, L. *Phys. Rev. Lett.* **2012**, *108*, 266803.
(14) Liu, L.; et al. *Sci. Rep.* **2013**, *3*, 1210.
(15) Castro Neto, A. H.; Peres, N. M. R.; Novoselov, K. S.; Geim, A. K. *Rev. Mod. Phys.* **2009**, *81*, 109.
(16) Giovannetti, G.; Khomyakov, P.; Brocks, G.; Karpan, V.; van den Brink, J.; Kelly, P. *Phys. Rev. Lett.* **2008**, *101*, 026803.
(17) Novoselov, K. S.; Geim, A. K.; Morozov, S. V.; Jiang, D.; Katsnelson, M. I.; Grigorieva, I. V.; Dubonos, S. V.; Firsov, A. A. *Nature* **2005**, *438*, 197.

(18) Uchoa, B.; Rappoport, T. G.; Castro Neto, A. H. *Phys. Rev. Lett.* **2011**, *106*, 016801.
(19) Jacob, D.; Kotliar, G. *Phys. Rev. B* **2010**, *82*, 085423.
(20) Li, L.; Ni, Y.-Y.; Zhong, Y.; Fang, T.-F.; Luo, H.-G. *New J. Phys.* **2013**, *15*, 053018.
(21) Krychowski, D.; Kaczkowski, J.; Lipinski, S. *Phys. Rev. B* **2014**, *89*, 035424.
(22) Wehling, T. O.; Balatsky, A. V.; Katsnelson, M. I.; Lichtenstein, A. I.; Rosch, A. *Phys. Rev. B* **2010**, *81*, 115427.
(23) Eelbo, T.; Wasniowska, M.; Gyamfi, M.; Forti, S.; Starke, U.; Wiesendanger, R. *Phys. Rev. B* **2013**, *87*, 205443.
(24) Wang, Y.; Brar, V. W.; Shytov, A. V.; Wu, Q.; Regan, W.; Tsai, H. Z.; Zettl, A.; Levitov, L. S.; Crommie, M. F. *Nat. Phys.* **2012**, *8*, 653.
(25) Brar, V. W.; et al. *Nat. Phys.* **2011**, *7*, 43.
(26) Donati, F.; Dubout, Q.; Autès, G.; Patthey, F.; Calleja, F.; Gambardella, P.; Yazyev, O. V.; Brune, H. *Phys. Rev. Lett.* **2013**, *111*, 236801.
(27) Kresse, G.; Furthmüller, J. *Comput. Mater. Sci.* **1996**, *6*, 15.
(28) Blöchl, P. E. *Phys. Rev. B* **1994**, *50*, 17953.
(29) Perdew, J. P.; Zunger, A. *Phys. Rev. B* **1981**, *23*, 5048.
(30) Pan, Y.; Zhang, H. G.; Shi, D. X.; Sun, J. T.; Du, S. X.; Liu, F.; Gao, H. J. *Adv. Mater.* **2009**, *21*, 2777.
(31) Pan, Y.; Shi, D. X.; Gao, H. J. *Chin. Phys.* **2007**, *16*, 3151.
(32) Prüser, H.; et al. *Nat. Phys.* **2011**, *7*, 203.
(33) Fano, U. *Phys. Rev.* **1961**, *124*, 1866.
(34) Frota, H. O. *Phys. Rev. B* **1992**, *45*, 1096.
(35) Costi, T. A. *Phys. Rev. Lett.* **2000**, *85*, 1504.
(36) Mao, J. H.; et al. *Appl. Phys. Lett.* **2012**, *100*, 182104.
(37) Tersoff, J.; Hamann, D. R. *Phys. Rev. B* **1985**, *31*, 805.

dx.doi.org/10.1021/nl501425n | *Nano Lett.* 2014, 14, 4011−4015